

One-step hydrothermal synthesis of porous $\text{Ti}_3\text{C}_2\text{T}_z$ MXene/rGO gels for supercapacitor applications

Sanjit Saha¹, Kailash Arole², Miladin Radovic,² Jodie L. Lutkenhaus,^{1,2*} Micah J. Green^{1,2*}

¹Artie McFerrin Department of Chemical Engineering, Texas A&M University, College Station, TX 77843, USA

²Department of Materials Science and Engineering, Texas A&M University, College Station, TX 77843, USA

*Corresponding authors: micah.green@tamu.edu; jodie.lutkenhaus@tamu.edu

Supporting Information

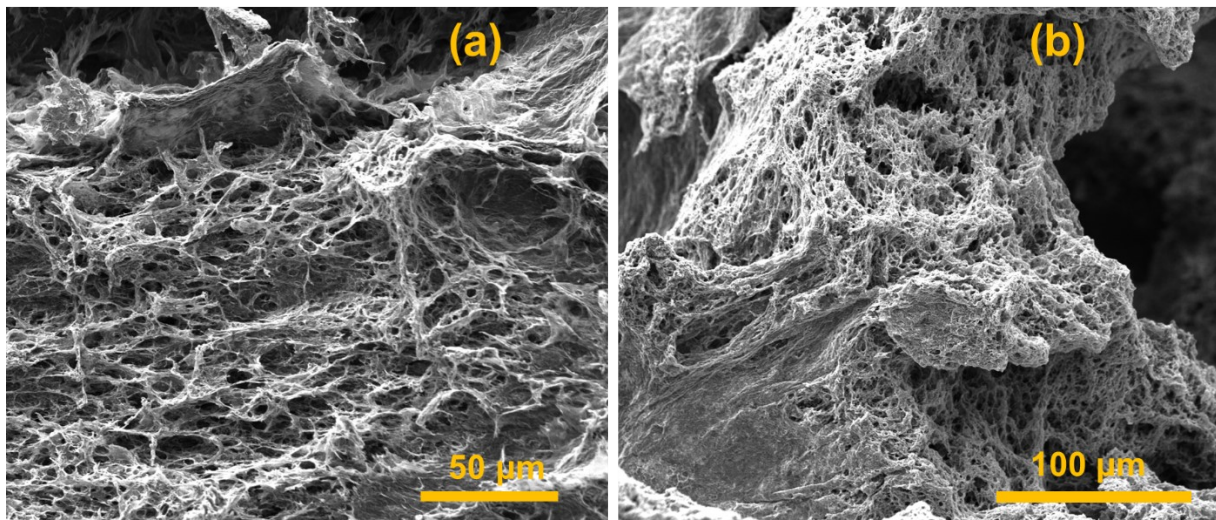


Figure S1. FE-SEM images of GM2 shows porous structure favorable for transportation of electrolyte ions

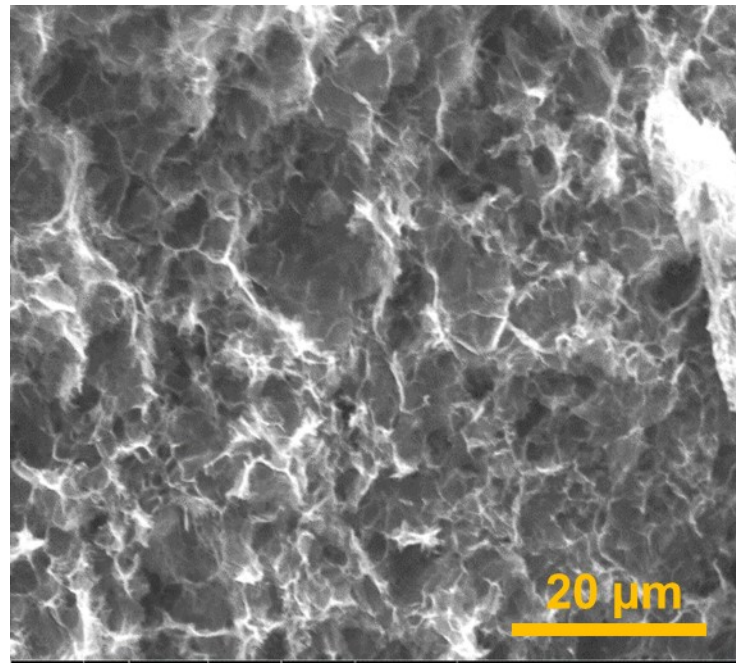


Figure S2. FE-SEM images of GM0

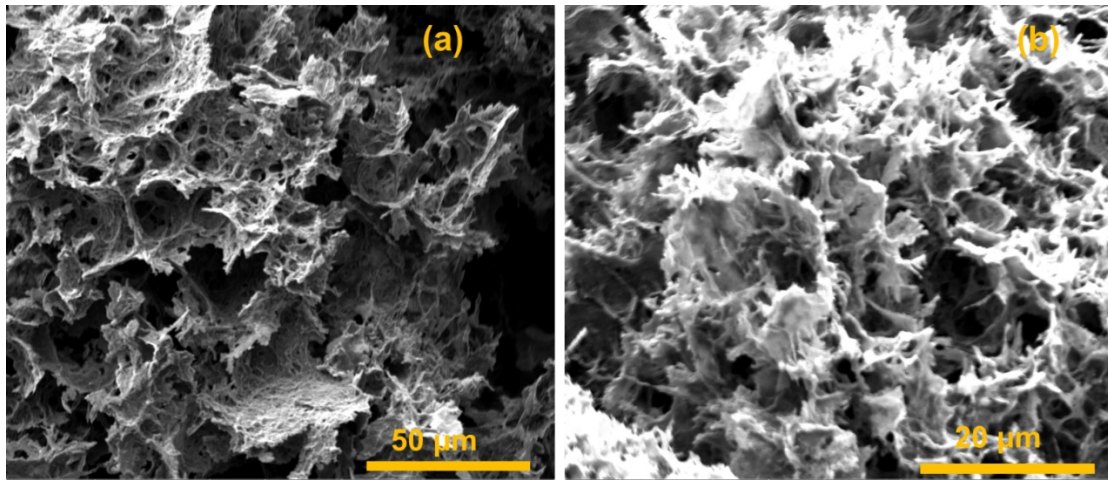


Figure S3. FE-SEM images of (a) GM1 and (b) GM3

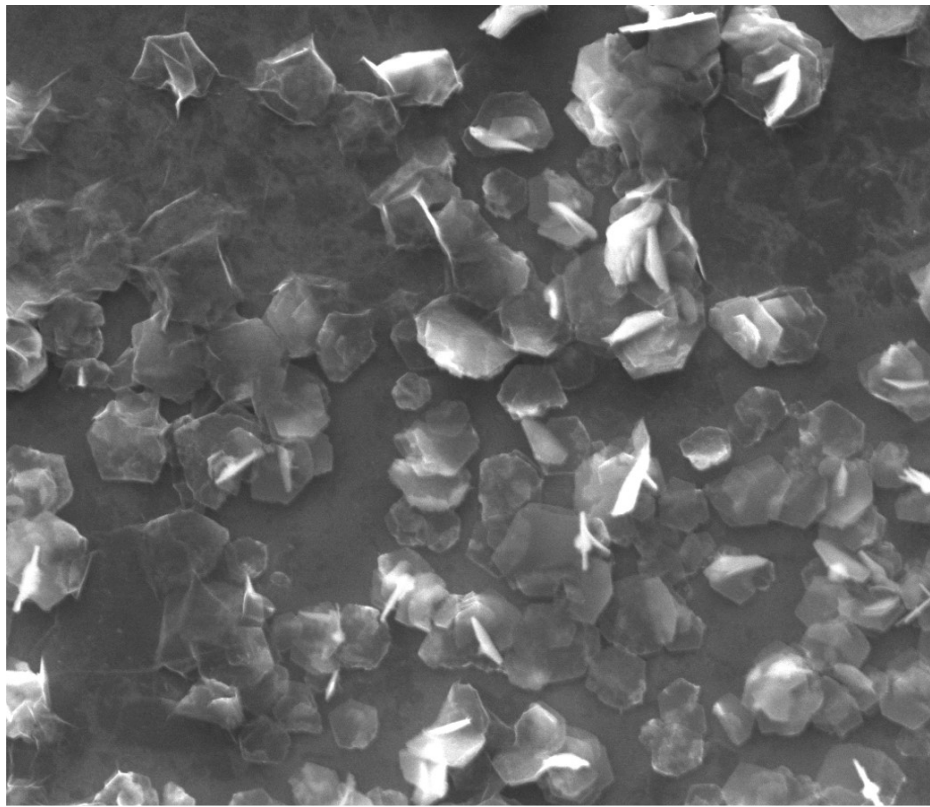


Figure S4. FE-SEM images of Ti₃C₂T_z nanosheets

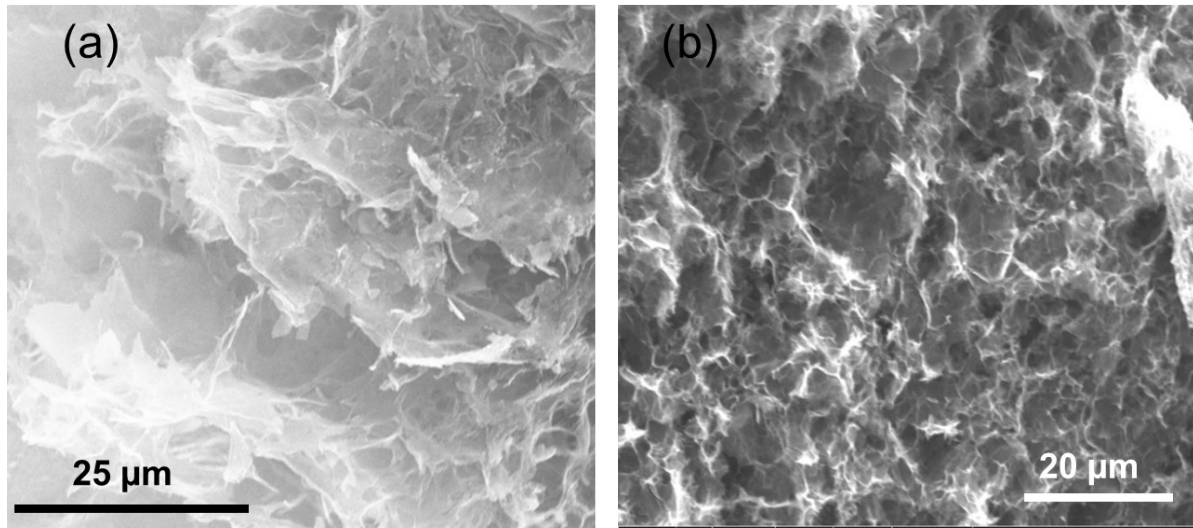


Figure S5. FE-SEM of GM2 and GM0 for EDS analysis

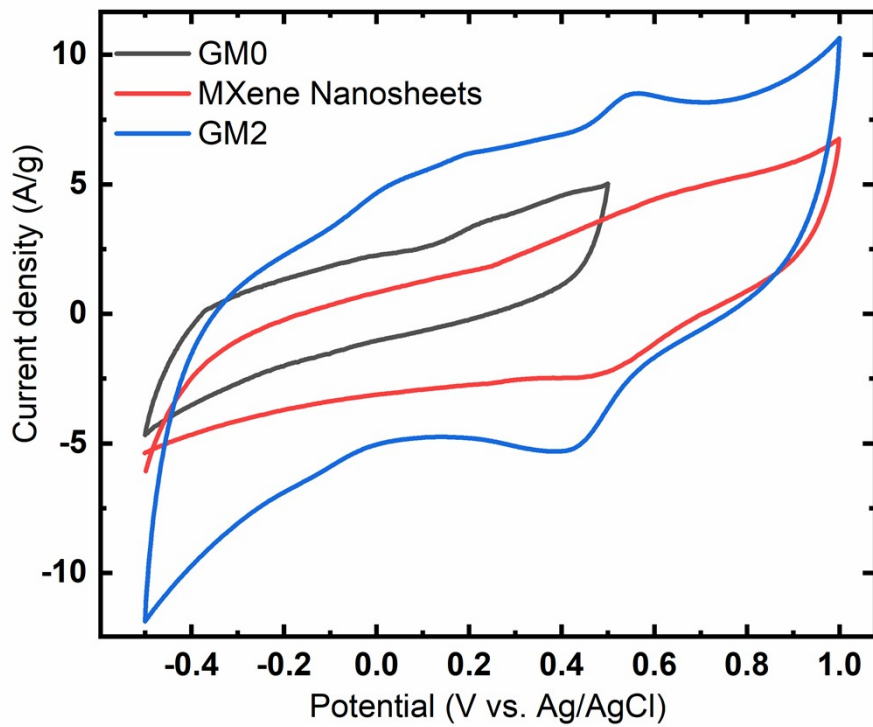


Figure S6. Three electrode CV of pure rGO gel (GM0), $\text{Ti}_3\text{C}_2\text{T}_z$ Nanosheets and $\text{Ti}_3\text{C}_2\text{T}_z$ /rGO gel (GM2) at 10 mV/s scan rate. The specific capacitance was calculated as 314, 402 and 920 F/g for GM0, $\text{Ti}_3\text{C}_2\text{T}_z$ nanosheets and GM2, respectively. The potential window of $\text{Ti}_3\text{C}_2\text{T}_z$ /rGO (1.5 V) is higher than pure rGO gel.

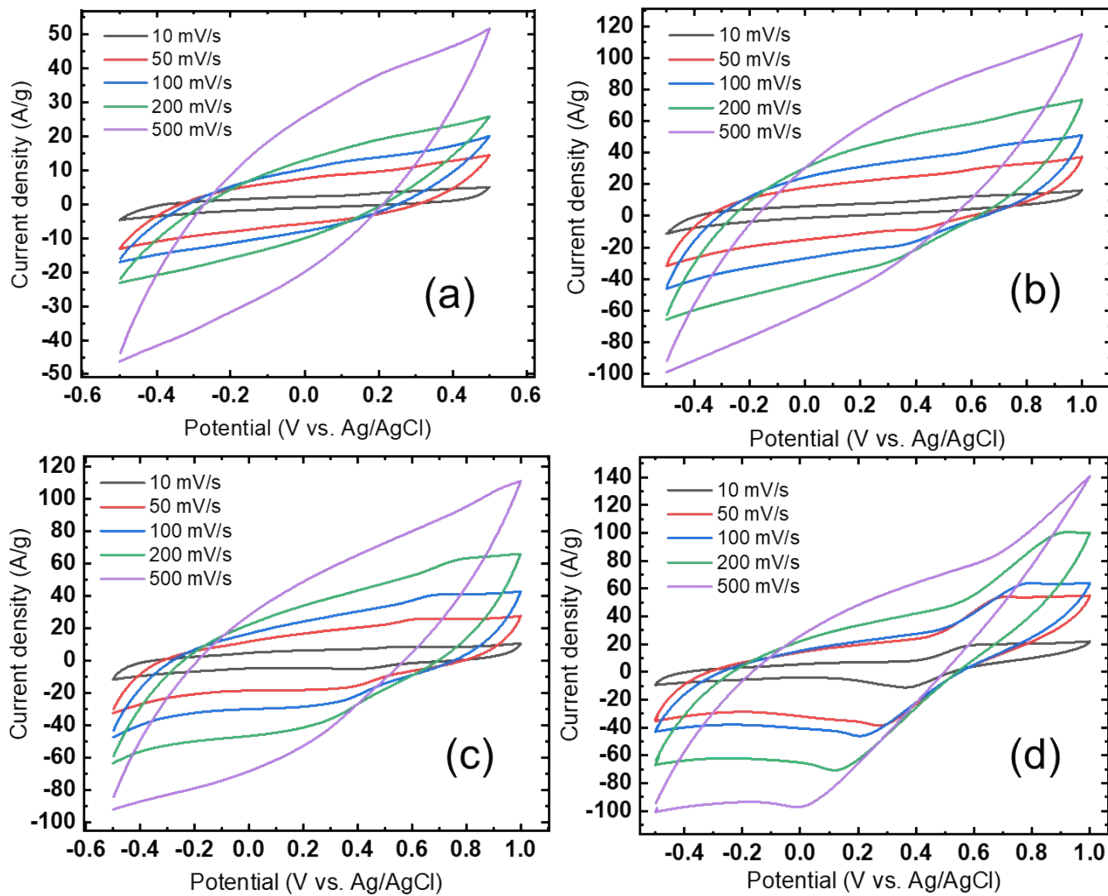


Figure S7. CV of (a) GM0, (b) GM1, (c) GM2, and (d) GM3 at different scan rates. The CV plots show appearance of redox peak with higher $\text{Ti}_3\text{C}_2\text{T}_z$ content (GM2 and GM3). At high scan rate the CV nature of GM2 is stable but GM3 got distorted due to excess $\text{Ti}_3\text{C}_2\text{T}_z$ content.

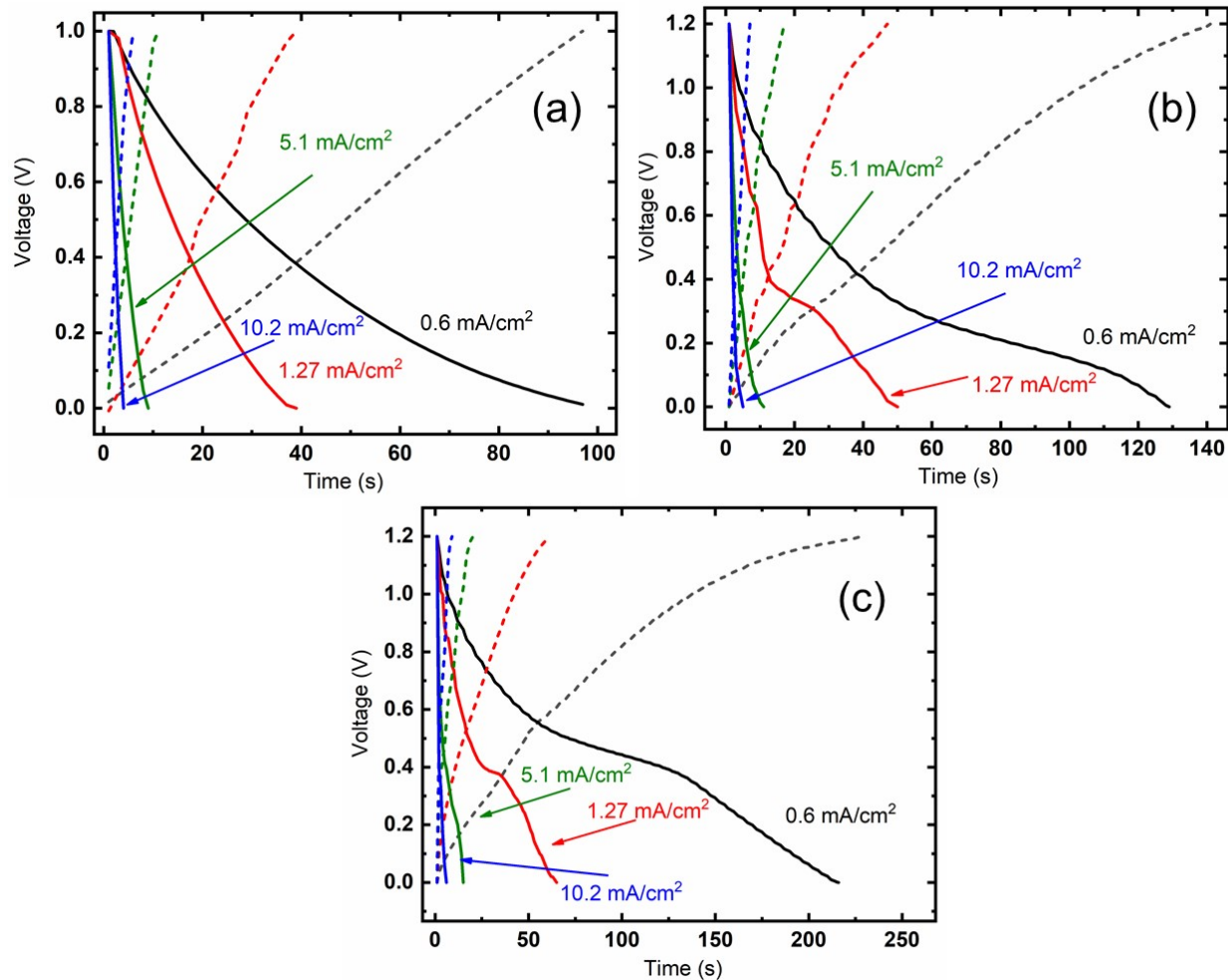


Figure S8. Two-electrode CD of (a) GM0, (b) GM1, and (c) GM3 at different current densities. The discharging time of the symmetric cells constructed with $\text{Ti}_3\text{C}_2\text{T}_z$ /rGO gels is significantly higher than the pure rGO symmetric cell.

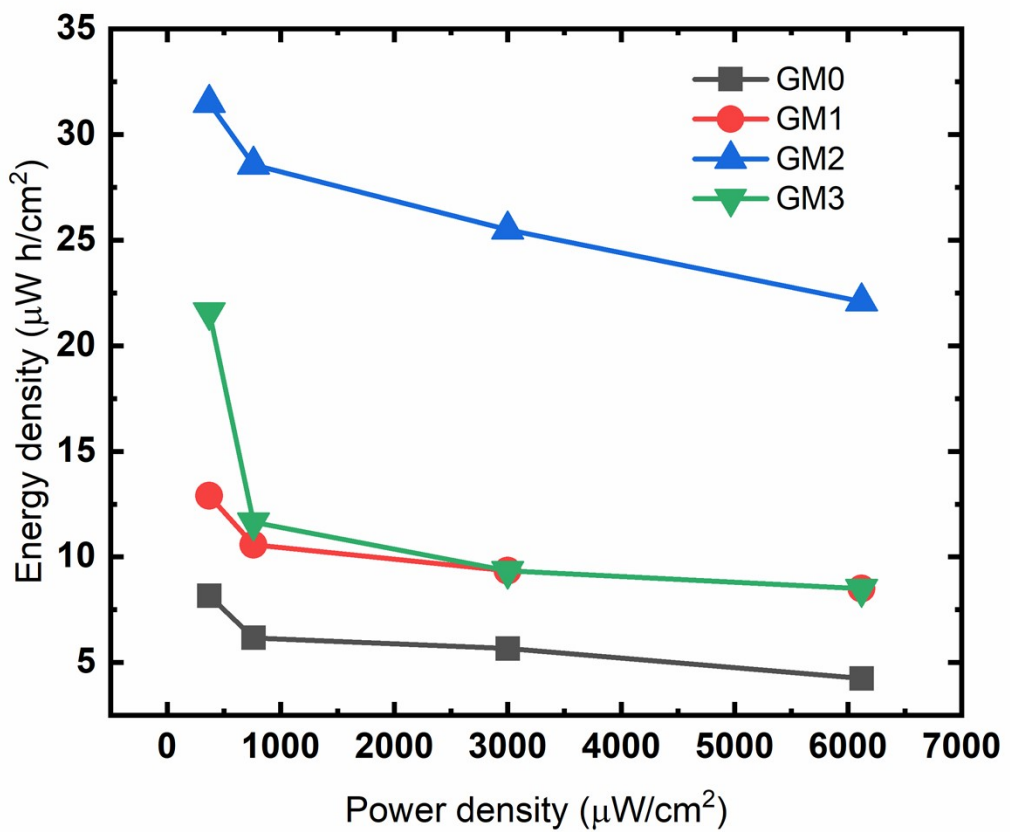


Figure S9. Ragone plot of GM0, GM1, GM2 and GM3 two electrode supercapacitor cell. GM2 shows higher energy density than both GM1 and GM3.

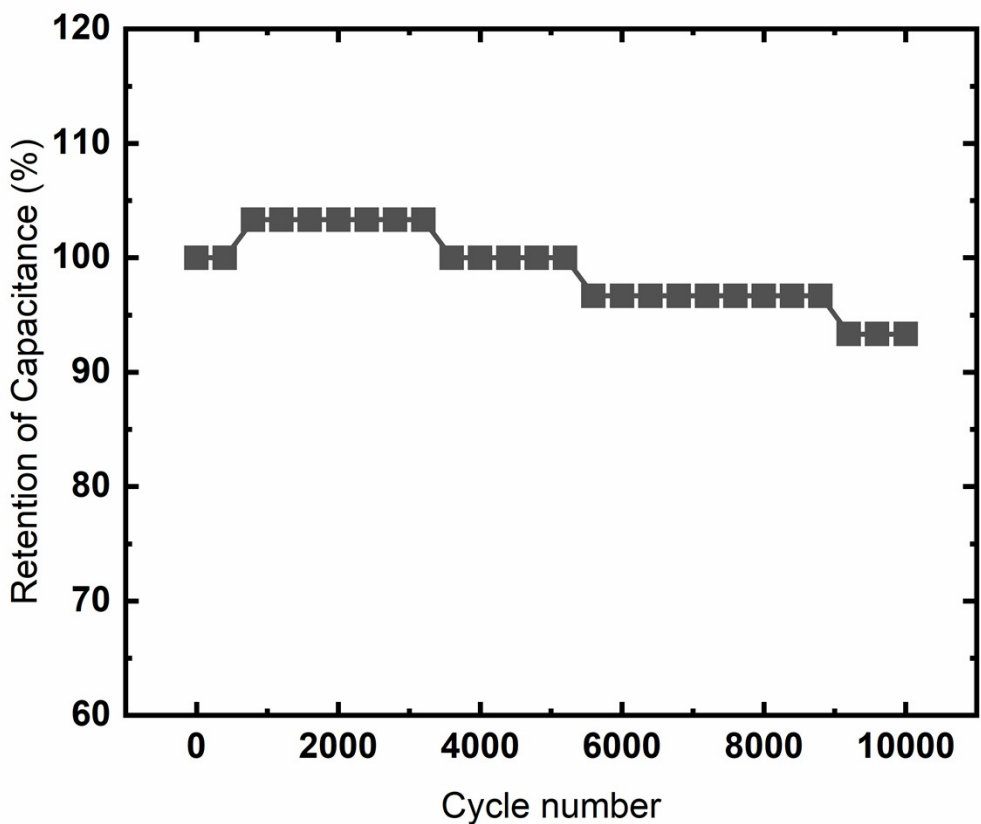


Figure S10. Stability study of GM2 two electrode supercapacitor at a current density of 5.1 mA/cm². GM2 (symmetric cell) shows ~93% retention after, 10,000 cycles.

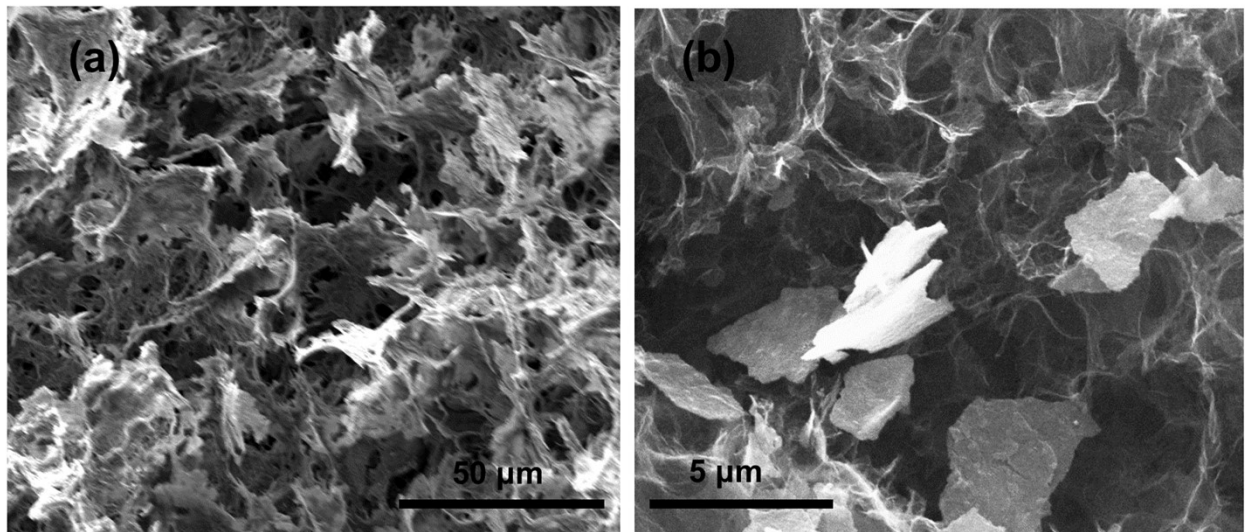


Figure S11. (a) Low- and (b) high-magnification FE-SEM image of $\text{Ti}_3\text{C}_2\text{T}_z/\text{rGO}$ gel after charge discharge 10000 cycles. $\text{Ti}_3\text{C}_2\text{T}_z/\text{rGO}$ gel after 10000 cycles shows a highly porous structure, similar to the un-used $\text{Ti}_3\text{C}_2\text{T}_z/\text{rGO}$.

Table S1. Comparison of the surface area of different graphene and graphene/MXene gel.

Material	Surface area (m ² /g)	Reference
MXene-Derived TiO ₂ @rGO	174	¹
Ti ₃ C ₂ Tx/GO hydrogel	65	²
MXene/Graphene hydrogel	161.1	³
Graphene Aerogels	350	⁴
Graphene Aerogel	516	⁵
Graphene oxide Aerogel	745	⁶
N-doped graphene aerogel	446	⁷
CNT/Graphene Aerogel	435	⁸
MXene/rGO gel	224	Present work

Table S2. Comparison of the specific capacitance (three electrode) of graphene and MXene electrode with the present work. The specific capacitance of MXene/rGO gel is significantly higher than pure rGO and MXene electrode.

	Specific capacitance (F/g)	Scan rate (mV/s)	References
Few-layer graphene	180	60	9
Highly corrugated graphene	349	2	10
Graphene nano-platelet	214	10	11
KOH modified graphene	136	10	12
Graphene Aerogel	176	1 A /g	13
Ti ₃ C ₂ T _x clay	246	2	14
Ti ₃ C ₂ T _x	67.7	1 A /g	15
Surface-modified 2D titanium carbide	325	2	16
MXene/rGO gel	920	10	Present work

Table S3. Comparison of the specific capacitance, energy density, power density and stability (two electrode) of graphene and MXene electrode with the present work

	Specific capacitance (mF/cm ²)	Energy density (μW h/cm ²)	Corresponding Power density (μW/cm ²)	Stability (after 10,000 cycles)	References
3D graphene	18.70	2.59	230	93%	17
Hydrothermally reduced GO	38.2	5.3			18
rGO/CNT	269	5.91	20		19
3D MXene	2.1	24.4	640	90%	20
Additive-free MXene	562 F/cm ³	0.32	11.4	97%	21
Carbon//MXene	52	2.62	1620	86% (after 5,000 cycles)	22
Co-Al-LDH/MXene	40	8.84	230	92%	23
3D vanadium nitride (VN) nanowire/CNT	213.5	96	270	96.8% (after 5,000 cycles)	24
Graphene/titanium carbide aerogel	171.4	2.1	301.2	93%	25
3D MXene–Graphene Aerogel	34.6	2.18	60	91% (after 15,000 cycles)	26
MXene/rGO gel	158	31.5	360	93%	Present work

REFERENCES

1. Fang, Y.; Zhang, Y.; Miao, C.; Zhu, K.; Chen, Y.; Du, F.; Yin, J.; Ye, K.; Cheng, K.; Yan, J.; Wang, G.; Cao, D., MXene-Derived Defect-Rich TiO₂@rGO as High-Rate Anodes for Full Na Ion Batteries and Capacitors. *Nano-Micro Letters* **2020**, 12 (1), 128.
2. Chen, Y.; Xie, X.; Xin, X.; Tang, Z.-R.; Xu, Y.-J., Ti3C2Tx-Based Three-Dimensional Hydrogel by a Graphene Oxide-Assisted Self-Convergence Process for Enhanced Photoredox Catalysis. *ACS Nano* **2019**, 13 (1), 295-304.
3. Zhang, L.; Or, S. W., Self-assembled three-dimensional macroscopic graphene/MXene-based hydrogel as electrode for supercapacitor. *APL Materials* **2020**, 8 (9), 091101.
4. Han, Z.; Tang, Z.; Shen, S.; Zhao, B.; Zheng, G.; Yang, J., Strengthening of Graphene Aerogels with Tunable Density and High Adsorption Capacity towards Pb²⁺. *Scientific Reports* **2014**, 4 (1), 5025.
5. Wu, X.; Lyu, J.; Hong, G.; Liu, X.-c.; Zhang, X., Inner Surface-Functionalized Graphene Aerogel Microgranules with Static Microwave Attenuation and Dynamic Infrared Shielding. *Langmuir* **2018**, 34 (30), 9004-9014.
6. Luan, V. H.; Tien, H. N.; Hoa, L. T.; Hien, N. T. M.; Oh, E.-S.; Chung, J.; Kim, E. J.; Choi, W. M.; Kong, B.-S.; Hur, S. H., Synthesis of a highly conductive and large surface area graphene oxide hydrogel and its use in a supercapacitor. *Journal of Materials Chemistry A* **2013**, 1 (2), 208-211.
7. Xu, P.; Gao, Q.; Ma, L.; Li, Z.; Zhang, H.; Xiao, H.; Liang, X.; Zhang, T.; Tian, X.; Liu, C., A high surface area N-doped holey graphene aerogel with low charge transfer resistance as high performance electrode of non-flammable thermostable supercapacitors. *Carbon* **2019**, 149, 452-461.
8. Sui, Z.; Meng, Q.; Zhang, X.; Ma, R.; Cao, B., Green synthesis of carbon nanotube-graphene hybrid aerogels and their use as versatile agents for water purification. *Journal of Materials Chemistry* **2012**, 22 (18), 8767-8771.
9. Li, Z. J.; Yang, B. C.; Zhang, S. R.; Zhao, C. M., Graphene oxide with improved electrical conductivity for supercapacitor electrodes. *Applied Surface Science* **2012**, 258 (8), 3726-3731.
10. Yan, J.; Liu, J.; Fan, Z.; Wei, T.; Zhang, L., High-performance supercapacitor electrodes based on highly corrugated graphene sheets. *Carbon* **2012**, 50 (6), 2179-2188.
11. Obeidat, A. M.; Luthra, V.; Rastogi, A. C., Solid-state graphene-based supercapacitor with high-density energy storage using ionic liquid gel electrolyte: electrochemical properties and performance in storing solar electricity. *Journal of Solid State Electrochemistry* **2019**, 23 (6), 1667-1683.
12. Li, Y.; van Zijl, M.; Chiang, S.; Pan, N., KOH modified graphene nanosheets for supercapacitor electrodes. *Journal of Power Sources* **2011**, 196 (14), 6003-6006.
13. Chen, W.; Gui, D.; Liu, C.; Xiong, W.; Cai, X.; Tan, G.; Li, S.; Liu, J. In *Preparation of graphene aerogel and its electrochemical properties as the electrode materials for supercapacitors*, 2015 16th International Conference on Electronic Packaging Technology (ICEPT), 11-14 Aug. 2015; 2015; pp 35-38.
14. Ghidiu, M.; Lukatskaya, M. R.; Zhao, M. Q.; Gogotsi, Y.; Barsoum, M. W., Conductive two-dimensional titanium carbide 'clay' with high volumetric capacitance. *Nature* **2014**, 516 (7529), 78-81.
15. Zang, X.; Wang, J.; Qin, Y.; Wang, T.; He, C.; Shao, Q.; Zhu, H.; Cao, N., Enhancing Capacitance Performance of Ti3C2Tx MXene as Electrode Materials of Supercapacitor: From Controlled Preparation to Composite Structure Construction. *Nano-Micro Letters* **2020**, 12 (1), 77.
16. Dall'Agnese, Y.; Lukatskaya, M. R.; Cook, K. M.; Taberna, P.-L.; Gogotsi, Y.; Simon, P., High capacitance of surface-modified 2D titanium carbide in acidic electrolyte. *Electrochemistry Communications* **2014**, 48, 118-122.

17. Wang, Y.; Zhang, Y.; Liu, J.; Wang, G.; Pu, F.; Ganesh, A.; Tang, C.; Shi, X.; Qiao, Y.; Chen, Y.; Liu, H.; Kong, C.; Li, L., Boosting areal energy density of 3D printed all-solid-state flexible microsupercapacitors via tailoring graphene composition. *Energy Storage Materials* **2020**, *30*, 412-419.
18. Veerasubramani, G. K.; Krishnamoorthy, K.; Pazhamalai, P.; Kim, S. J., Enhanced electrochemical performances of graphene based solid-state flexible cable type supercapacitor using redox mediated polymer gel electrolyte. *Carbon* **2016**, *105*, 638-648.
19. Kou, L.; Huang, T.; Zheng, B.; Han, Y.; Zhao, X.; Gopalsamy, K.; Sun, H.; Gao, C., Coaxial wet-spun yarn supercapacitors for high-energy density and safe wearable electronics. *Nature Communications* **2014**, *5* (1), 3754.
20. Yang, W.; Yang, J.; Byun, J. J.; Moissinac, F. P.; Xu, J.; Haigh, S. J.; Domingos, M.; Bissett, M. A.; Dryfe, R. A. W.; Barg, S., 3D Printing of Freestanding MXene Architectures for Current-Collector-Free Supercapacitors. *Advanced Materials* **2019**, *31* (37), 1902725.
21. Zhang, C.; McKeon, L.; Kremer, M. P.; Park, S.-H.; Ronan, O.; Seral-Ascaso, A.; Barwick, S.; Coileáin, C. Ó.; McEvoy, N.; Nerl, H. C.; Anasori, B.; Coleman, J. N.; Gogotsi, Y.; Nicolosi, V., Additive-free MXene inks and direct printing of micro-supercapacitors. *Nature Communications* **2019**, *10* (1), 1795.
22. Wang, N.; Liu, J.; Zhao, Y.; Hu, M.; Qin, R.; Shan, G., Laser-Cutting Fabrication of Mxene-Based Flexible Micro-Supercapacitors with High Areal Capacitance. *ChemNanoMat* **2019**, *5* (5), 658-665.
23. Xu, S.; Dall'Agnese, Y.; Wei, G.; Zhang, C.; Gogotsi, Y.; Han, W., Screen-printable microscale hybrid device based on MXene and layered double hydroxide electrodes for powering force sensors. *Nano Energy* **2018**, *50*, 479-488.
24. Zhang, Q.; Wang, X.; Pan, Z.; Sun, J.; Zhao, J.; Zhang, J.; Zhang, C.; Tang, L.; Luo, J.; Song, B.; Zhang, Z.; Lu, W.; Li, Q.; Zhang, Y.; Yao, Y., Wrapping Aligned Carbon Nanotube Composite Sheets around Vanadium Nitride Nanowire Arrays for Asymmetric Coaxial Fiber-Shaped Supercapacitors with Ultrahigh Energy Density. *Nano Letters* **2017**, *17* (4), 2719-2726.
25. N, R.; A, K.; H.M, M.; M.R, N.; Mondal, D.; Nataraj, S. K.; Ghosh, D., Binder free self-standing high performance supercapacitive electrode based on graphene/titanium carbide composite aerogel. *Applied Surface Science* **2019**, *481*, 892-899.
26. Yue, Y.; Liu, N.; Ma, Y.; Wang, S.; Liu, W.; Luo, C.; Zhang, H.; Cheng, F.; Rao, J.; Hu, X.; Su, J.; Gao, Y., Highly Self-Healable 3D Microsupercapacitor with MXene–Graphene Composite Aerogel. *ACS Nano* **2018**, *12* (5), 4224-4232.